06

# Optical, electrical and EMI shielding properties of AgNW thin films

© A.S. Voronin,[1,2,3] I.I. Bril,[2] Y.V. Fadeev,[1,2] A.Y. Pavlikov,[3] M.M. Simunin,[2,3] M.N. Volochaev,[4] I.V. Govorun,[4] I.V. Podshivalov,[4] M.O. Makeev,[1] P.A. Mikhalev,[1] B.A. Parshin,[1] S.V. Khartov[2]

[1] Bauman Moscow State Technical University,
105005 Moscow, Russia
[2] Krasnoyarsk Scientific Center of the Siberian Branch of the Russian Academy of Sciences,
660036 Krasnoyarsk, Russia
[3] Siberian Federal University,
660041 Krasnoyarsk, Russia
[4] Kirensky Institute of Physics, Federal Research Center KSC SB, Russian Academy of Sciences,
660036 Krasnoyarsk, Russia
e-mail: a.voronin1988@mail.ru, ellaijiah@gmail.com

*Received July 10, 2024*
*Revised October 30, 2024*
*Accepted October 30, 2024*

This paper describes the process of obtaining silver nanowires (AgNW) and the technique for producing thin films on their basis using vacuum filtration. The film thickness was specified by the volume of the base dispersion. In order to improve the physical, mechanical and adhesive properties of the films, AgNW were integrated into a polyurethane substrate. Comprehensive studies of the morphology and structure of both individual AgNWs and their films were conducted. The study of the optoelectric characteristics showed that the AgNW films have a uniform transmittance in the visible range above 500 nm. The radio shielding properties of the film structures in the K and $K_a$- ranges were also studied. It was shown that the AgNW films have a high shielding coefficient of more than 25 dB in the entire studied frequency range, while the optical transmittance at a wavelength of 550 nm was 69.25%.

**Keywords:** Silver nanowires, AgNW, shielding efficiency, thin films, electrical properties, optical properties.

DOI: 10.61011/TP.2025.01.60512.224-24

## Introduction

The modern world cannot be imagined without the widespread use of electronic devices. The amount of electronics used in the military, medical, commercial and civilian industries is growing as the industry develops [1]. However, all electronics generate unwanted electromagnetic interference (EMI). This parasitic radiation has a negative impact on the stable operation of electronics, causing both temporary malfunctions and critical problems in the operation of devices [2,3]. In addition, back in the last century, the possibility of intercepting side radiation from a monitor screen with its subsequent decoding was shown [4]. Subsequently, this information leak channel was abbreviated TEMPEST [5,6]. Given that the visual channel is the primary used electronic communication channel [7], the demand for research in the field of optically transparent coatings that protect from EMF is growing every year [8]. Two types of transparent shielding coatings are most often used in the literature. The first type comprises metal meshes with a period of $500-1000\,\mu$m and a track width of $25-50\,\mu$m. They have a high shielding efficiency (over 50 dB) at frequencies below 1 GHz. However, the shielding efficiency of metal meshes significantly decreases at frequencies above 1 GHz. For example, it is reported in Ref. [9] that a shielding efficiency of a metal mesh with a cell size of 1.2 mm will not exceed 10 dB at a frequency of 26 GHz. The second type comprises transparent conductive oxides, which are abbreviated as TCO (Transparent Conductive Oxides) in the foreign literature. Indium tin oxide (ITO) is a typical representative of this type of coating, its shielding efficiency is practically independent of frequency and is at the level of 20 dB in the frequency band from 1 to 40 GHz [10]. Silver nanowires are an excellent candidate for an optically transparent shielding material [11]. For example, it is reported in Ref. [12] about AgNW films with an optical transparency of about 85% with a shielding capacity of $20-25$ dB depending on the operating frequency, which exceeds the results shown in the studies of ITO films. We see similar results in the papers [13–15]. These studies, as well as the issue of the shielding properties of AgNW at frequencies outside the X-band, which has not been disclosed in modern literature, prompted us to study the spectral characteristics of silver nanowire thin films in a wide frequency range corresponding to 5G, which includes the K- and $K_a$-bands.

## 1. Materials and methods

### 1.1. Synthesis of silver nanowires

Ultra-long silver AgNW nanowires were synthesized using solvothermal method: first, 0.3 g of polyvinylpyrrolidone(PVP) (M.W. — 1.3 MDa) and $AgNO_3$ (0.20 g,

1.18 mM) were dissolved in 50 m*l* of ethylene glycol. Then a solution of $FeCl_3$ (200 $\mu l$, 12.5 $\mu$M) was added and stirred at room temperature. The resulting mixture was then transferred to a Teflon-lined autoclave with a capacity of 50 m*l*. This mixture of reagents was kept at 130°C for 8 h until completion of the reaction. Solvent replacement operations were performed after synthesis of AgNW. The obtained solution in ethylene glycol was centrifuged for this purpose at a rate of 10 000 rpm for 15 min using laboratory centrifuge OPN 16 (Labtex, Russia). The supernatant was drained after centrifugation and the same amount of isopropyl alcohol was added. This operation was repeated 5 times until the complete removal of ethylene glycol, ions of $NO_3^-$, $Cl^-$ and $Fe^{3+}$ and PVP residues.

### 1.2. Production of AgNW films

AgNW thin films were produced using the vacuum filtration method [16]. The thickness of the AgNW films was determined by the dispersion volume. The basic AgNW dispersion with a nanowire concentration of 4 mg/m*l* was used in this study. The volumes of the basic dispersion used in the study for the production of films were 25, 50, 100, 200, 400, 800 and 1600 $\mu l$. The said volumes of the base dispersion were diluted with isopropyl alcohol to a volume of 50 m*l*. Acetate cellulose filters (MFAS-B-3, Vladipor, Russia) with a pore diameter of 600 nm and a working diameter of 20 mm were used for the filtration, the filtered wet AgNW film on the filter was pressed against the glass surface with a force of 10 kg/cm$^2$ and was dried at room temperature for 30 min. Subsequently, the system was immersed in acetone for dissolving the cellulose filter acetate and obtaining thin AgNW films on the glass. AgNW films were integrated into the surface layer of a flexible polyurethane substrate for obtaining wear-resistant films using the following method: first, a prepolymer of polyester diisocyanate-2,4 was mixed in butyl acetate together with methylene-bis-ortho-chloroaniline (MOCA) and degassed. Then the resulting solution was applied over AgNW films and polymerized in a drying cabinet with multi-stage heating in the following conditions: initially, the cabinet was heated to 50°C, then the temperature was adjusted to 100°C with a step of 10°C and holding for 1 h at each step. After reaching 100°C, the samples were kept at this temperature for 10 h.

### 1.3. Testing of adhesive properties

The adhesive properties of the AgNW film samples were determined by the cross-cut method (ASTM D4541) [17].

### 1.4. Optical and electron microscopy

Optical microscopy images were acquired using Altami 104 microscope (Altami, Russia). The morphology and geometric characteristics of single AgNW were studied by transmission electron microscopy (TEM) using HT 7700 (Hitachi, Japan) with an accelerating voltage of 40–300 kV. The morphology of AgNW films was studied by scanning electron microscopy (SEM) using SU3500 (Hitachi, Japan) microscope with an accelerating voltage of 20 kV.

### 1.5. X-ray diffraction analysis

X-ray images of the samples were taken using X'Pert Pro MPD diffractometer (PANalytical, Netherlands) with a high-speed PIXcel detector in the angular range of 30–90° 2Θ, with a step of 0.013°. The parameters of the Ag crystal lattice were determined using Rietveld full-profile approach by derivative difference minimization (DDM).

### 1.6. Measurement of optoelectric characteristics

The spectral dependences of the optical transmittance of AgNW films were measured in the range of 380–780 nm using UV-3600i Plus spectrophotometer with an integrating sphere (Shimadzu, Japan). The scattering ability of AgNW films was estimated using the Haze parameter. The Haze parameter is determined using the following formula according to the D1003 — 13„Standard Test Method for Haze and Luminous Transmittance of Transparent Plastics“:

$$\text{Haze}[\%] = T_d/T_t \cdot 100, \quad (1)$$

where $T_d$ is diffuse light transmittance, $T_t$ is total light transmittance.

The measurements consist of two stages: the transmittance of the sample is directly measured at the first stage— this is $T_r$. The transmittance in the sphere is measured at the second stage— this is $T_t$; then $T_d = T_t - T_r$ is calculated; the Haze parameter is calculated based on the obtained data.

The AgNW surface resistance was measured by four-probe method using Keithley 2000 multimeter (Keithley Instruments, USA) and a Mill-Max 854-22-004-10-001101 four-probe head (Mill-Max Mfg., USA).

### 1.7. Method for measuring the radio shielding properties of AgNW films

The waveguide method was used to evaluate the radio shielding properties of films. The sample was placed in the gap of the waveguide transmission line for this purpose, and the transmission ratio $S_{21}$ and reflection coefficient $S_{11}$ of the electromagnetic wave were measured. The measurements were conducted in two frequency bands: K-band (18–26.5 GHz) and $K_a$-band (26.5–40 GHz). The waveguide windows had a rectangular cross-section with dimensions of 4.3 × 10.65 mm for the K-band and 3.55 × 7.1 mm for the $K_a$-band. The measurements were conducted using vector network analyzer *R&S* ZVA 50 (GmbH & Co. KG, Germany).

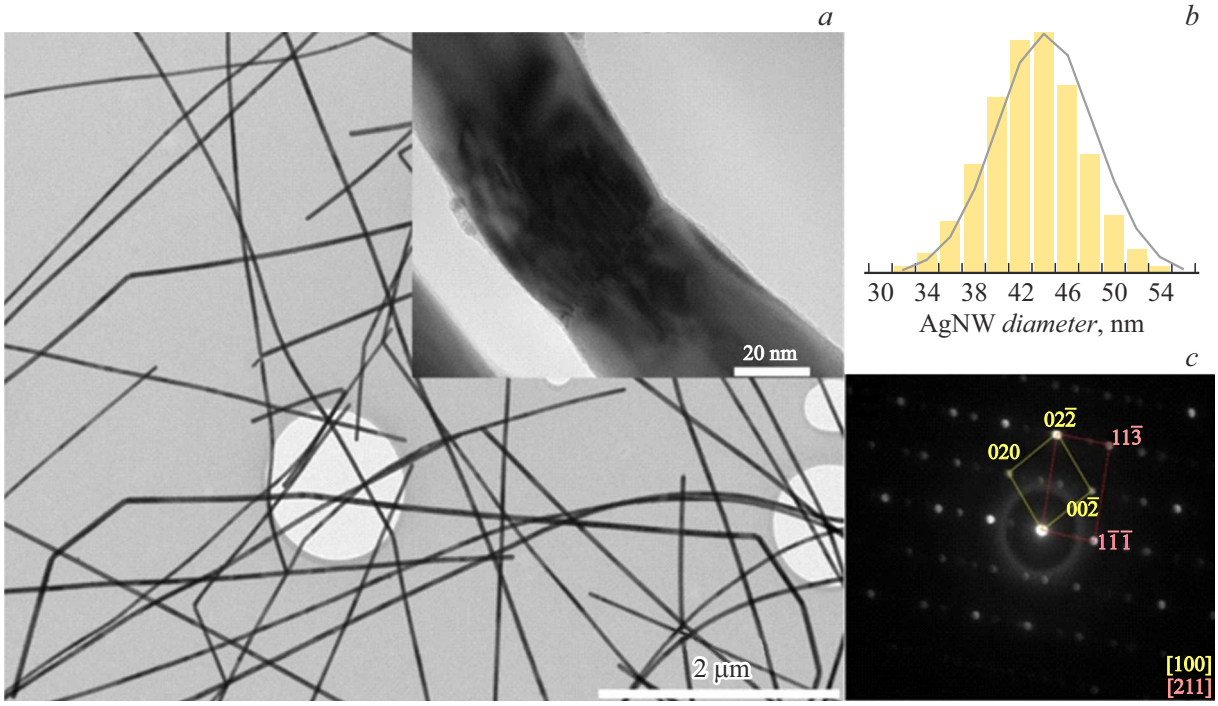


**Figure 1.** Morphological characteristics of synthesized silver nanowires: *a* — TEM images; *b* — normal distribution of nanowire diameters; *c* — selected area electron diffraction (SAED).

## 2. Results and discussion

### 2.1. Morphology and structure of AgNW and their films

The synthesized AgNW have a high aspect ratio. The wires have lengths of tens of micrometers with an average diameter of $43.2 \pm 12.4$ nm (Fig. 1, *a, b*). The adsorbed layer of macromolecules on the surface of nanowires comprises polyvinylpyrrolidone (PVP), adsorbed during AgNW synthesis (Fig. 1, *a*). PVP acts as a stabilizing agent in this case, preventing the agglomeration of nanowires and setting a preferential orientation in the growth process [18]. The diffraction of electrons from the selected zone (Fig. 1, *c*) indicates the twin structure of the obtained AgNW, which is found in the literature [19].

The UV-vis spectrum (Fig. 2, *a*) shows an absorption peak at a wavelength of 376 nm associated with plasmon resonance. This peak belongs to the transverse plasmon mode, and the position of the absorption peak is associated with the nanowire diameter. Thus, the position of the absorption peak for nanowires with a diameter of $43.2 \pm 12.4$ nm is in the range of 370–380 nm according to [20], which confirms our experimental results. The presence of a satellite peak at a wavelength of 356 nm is consistent with the literature and is associated with the excitation of a longitudinal plasmon mode, the wavelength of which is close to the wavelength of the surface plasmon for silver [21,22].

Two phases of silver were detected by the X-ray diffraction analysis of AgNW (Fig. 2, *b*). One phase has a normal cubic lattice, characteristic of silver, with parameters $a = b = c = 4.0868(7)$ Å, belonging to the spatial group Fm3m (narrow peaks). Another phase has a tetragonally distorted lattice belonging to the space group F4/mmm and the lattice parameters $a = b = 4.058(3)$, $c = 4.164(8)$ Å (asymmetrically broadened peaks). The tetragonal distortion of AgNW is caused by mechanical stresses that occur during the growth process. This feature is described in detail in Ref. [23].

Next, we studied the morphology of AgNW films integrated into reactoplastic polyurethane(RPU). We obtain a percolated nanowire structure at any concentrations used (Fig. 3). The most noticeable change of AgNW packing density per unit area is observed in case of an increase of the concentration of the base dispersion from 25 to 200 $\mu l$ (Fig. 3, *a–d*). At the same time, the number of nanowires per unit area in a single layer remains visually similar (Fig. 3, *e, f*). This means that we increase the number of AgNW layers in the film with a further increase of concentration.

## 3. Optoelectric properties of AgNW films

The spectral dependence of the transmittance coefficient in the range of 380–780 nm for all obtained AgNW films is shown in Fig. 4, *a*. The transmittance coefficient shows a downward trend with the increase of the concentration

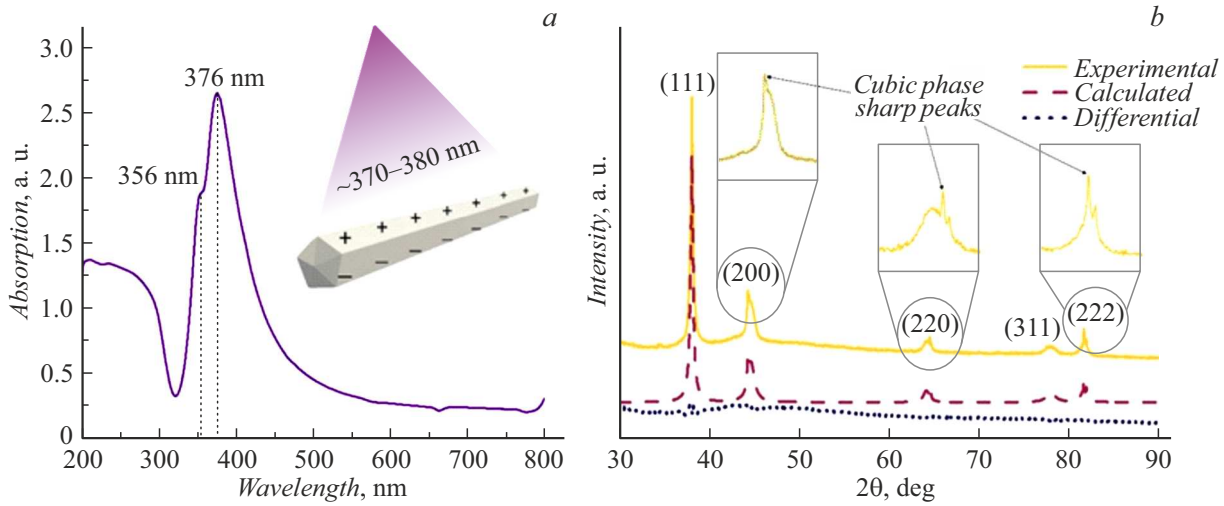


**Figure 2.** Morphological characteristics of synthesized silver nanowires: *a* — UV-vis absorption spectroscopy (the insert illustrates charge separation in AgNW during photon absorption); *b* — X-ray diffraction analysis data

of AgNW in the sample. Starting from the wavelength of $\sim 500$ nm, we observe a slope of the spectral line associated with plasmon absorption, which we also observed using UV-vis AgNW spectroscopy in solution. In general, the transmittance coefficient depends on the proportion of the surface coated with AgNW, which increases not only with the increase of the layer density, but also with the increase of the number of layers in the film [24]. Coatings with a concentration of basic dispersion of 25, 50, 100 $\mu l$ having optical transmittance at a wavelength of 550 nm, equal to 80.87, 73.81, 69.25%, respectively, are acceptable from the point of view of optoelectronics.

The turbidity value shows the ratio of diffuse light transmittance to total light transmittance. Since our films comprise a grid of randomly arranged AgNW, they easily disperse the incident radiation [25]. The turbidity index measured in our study (Fig. 4, *b*) does not exclude turbidity of the polyurethane substrate from RPU, which, judging by the literature data, is 3–5% [26]. Considering this, it is possible to note that samples with concentrations of 25, 50, and 100,$\mu l$ have an acceptable turbidity index for a transparent conductive film — at the level of 5–10%.

The surface resistance is directly dependent on the concentration of AgNW, which is consistent with the literature data [27]. A twofold increase of the concentration of the base dispersion results in an approximately twofold drop in surface resistance. The above-mentioned samples with base dispersion concentrations of 25, 50, and 100,$\mu l$ have surface resistances of 18.247, 12.138, and 4.917,Ω/sq, respectively. At the same time, we do not observe the effect of saturation of conductivity in case of the transition to the maximum studied concentration ($1600\,\mu l$) (Fig. 4, *c*). Considering this, it is possible to note that no transition from a quasi-two-dimensional structure to a three-dimensional structure takes place in our case [28].

It is advisable to study the relationship between the values of surface resistance and transmittance in the visible range for transparent conductive materials. We evaluated the relationship between these two parameters, by plotting the points corresponding to different concentrations of AgNW in films on a graph on which the axes are the transmittance coefficient and surface resistance (Fig. 4, *d*). The relationship between these two parameters, which are critically important for transparent conductors, is called the Figure of Merit (FoM). The equation for calculating the FoM is described in Ref. [29] and has the following form:

$$\mathrm{FoM} = \frac{Z_0}{2R\left(\frac{1}{\sqrt{T}} - 1\right)}, \tag{2}$$

where, $Z_0$ — vacuum impedance, $R$ — surface resistance of the coating, $T$ — transmittance coefficient.

We approximated the obtained points with a curve, according to equation (2), we obtained the best agreement for the FoM value equal to 210. For comparison, an ITO thin film on a flexible polyethylene terephthalate substrate is characterized by an FoM value of 115 [30].

### 3.1. Radio shielding properties of AgNW films

Radio shielding is an attenuation of an electromagnetic wave using a screen with high electrical conductivity [31]. It occurs due to losses on absorption and reflection of the incident wave [32]. The coefficients of reflection ($R$), transmittance ($T$) and absorption ($A$) can be expressed as

$$R[\%] = \frac{P_r}{P_i} = 10^{0.1S_{11}} \cdot 100, \tag{3}$$

$$T[\%] = \frac{P_t}{P_i} = 10^{0.1S_{21}} \cdot 100, \tag{4}$$

$$A[\%] = 100 - T - R, \tag{5}$$

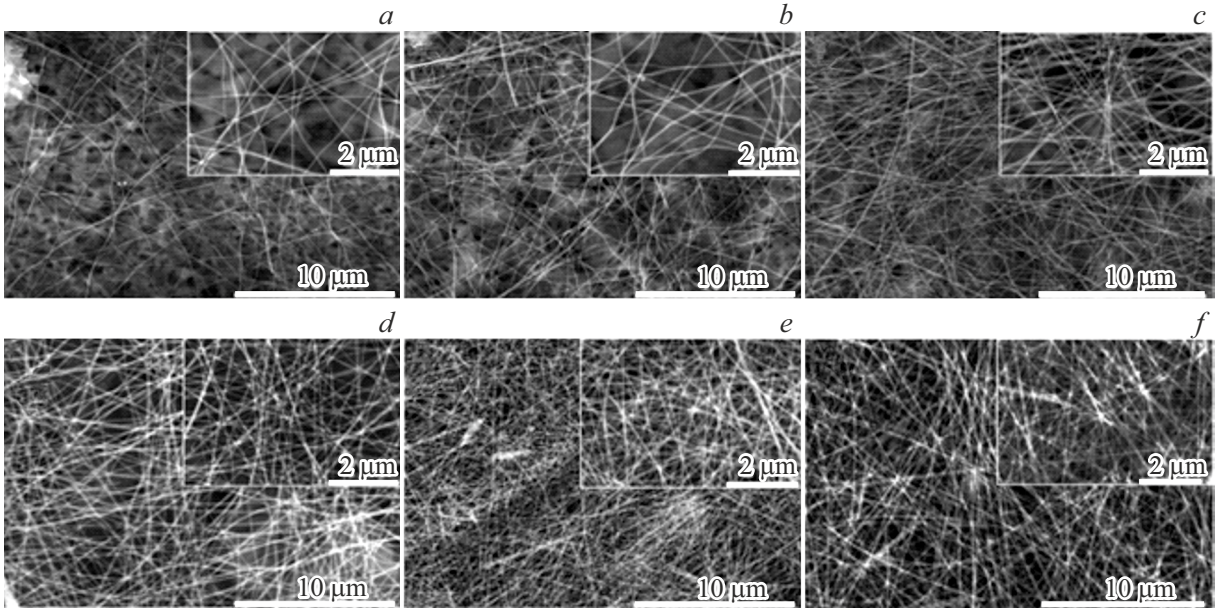


**Figure 3.** Scanning electron microscopy images of nanowires integrated into reactoplastic polyurethane: *a* — 25, *b* — 50, *c* — 100, *d* — 200, *e* — 400, *f* — 800 *μl*.

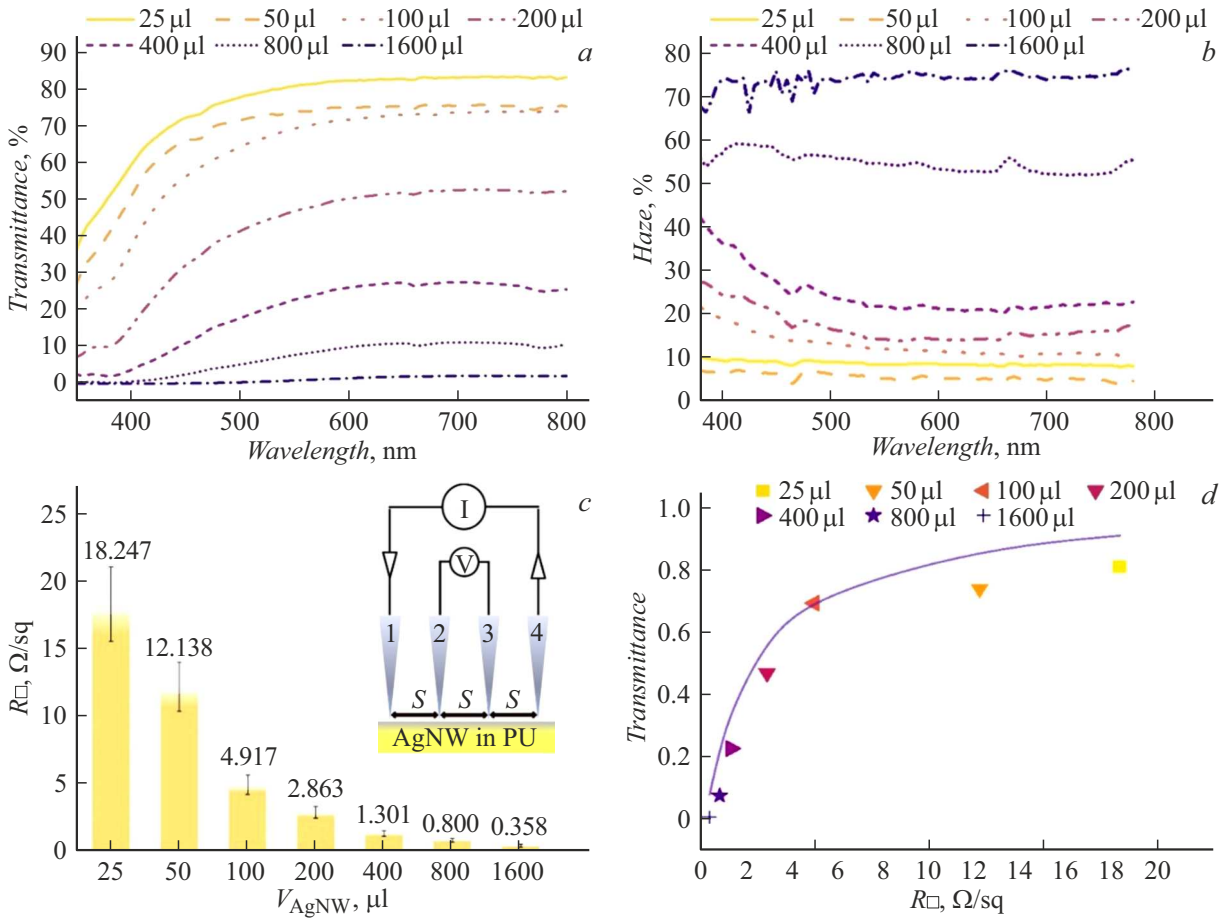


**Figure 4.** Optoelectric properties of AgNW films: *a* — transmittance coefficient; *b* — turbidity index; *c* — surface resistance (the insert illustrates the position of the measuring probes during the four-probe measurement, the distance between the probes $S = 2$ mm); *d* — Figure of Merit of AgNW films obtained.

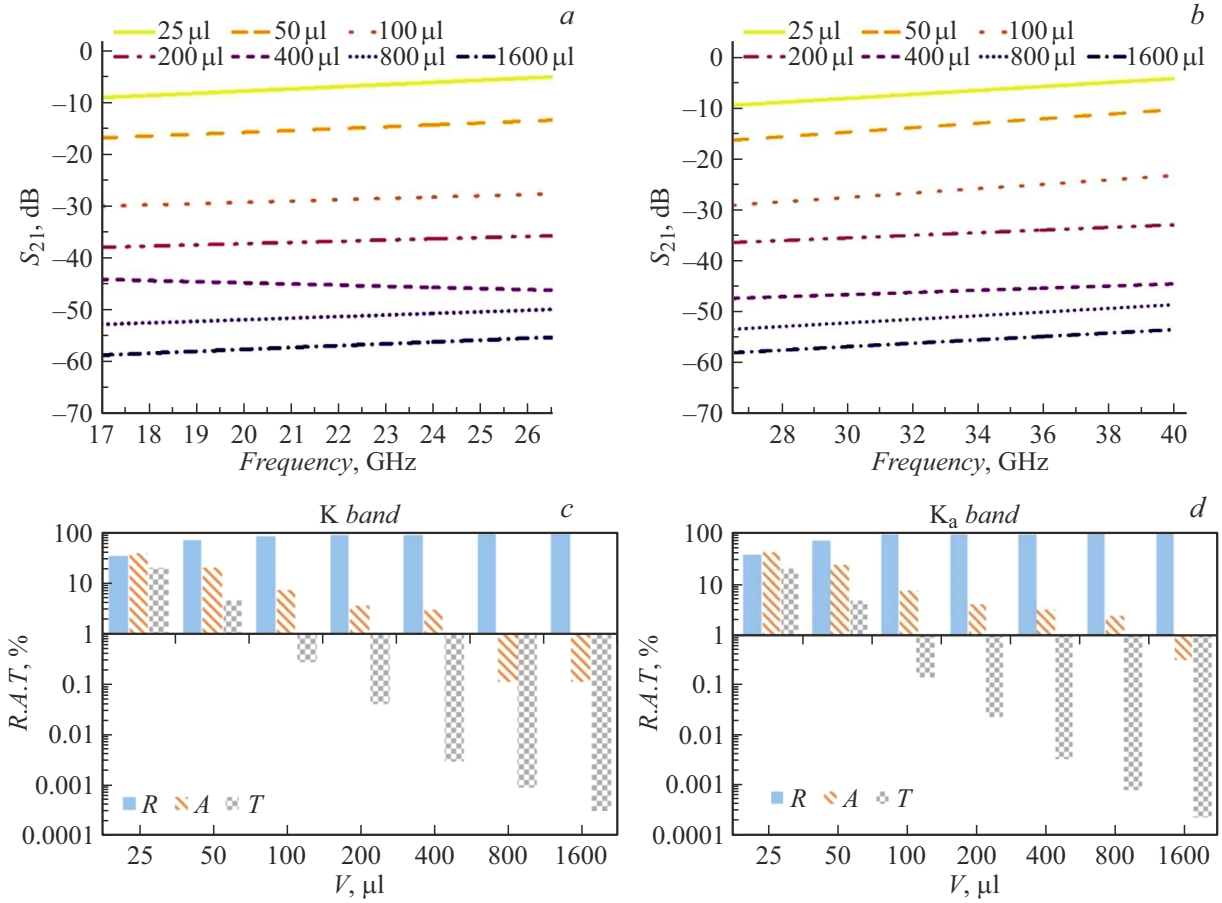


**Figure 5.** Radio shielding properties of AgNW films: *a, b* — transmittance coefficient $T$; *c, d* — histograms of the energy balance.

where $P_i$, $P_r$, $P_t$ are the powers of the incident, reflected, and transmitted waves, and $S_{21}$ and $S_{11}$ are the parameters of the dispersion matrix.

The shielding capacity can be estimated using the value of the shielding efficiency $SE$. The value of the shielding efficiency is related to the transmittance coefficient $T$ by the following equation:

$$SE = -10\log_{10}(S_{21}). \tag{6}$$

Fig. 5, *a, b* shows that the sample shielding efficiency depends on the concentration of AgNW. We observe a weak trend towards a decrease of shielding capacity with the increase of the frequency in all the studied ranges. Taking this into account, it is possible to characterize AgNW films in the studied bands using the average value of the transmittance coefficient. For example, a film from $100\,\mu l$ base dispersion with an optical transmittance coefficient of 69.25% and shielding efficiency $SE$ of 28.7 dB in the K-band and 26.0 dB in the $K_a$-band, respectively, is an optimal sample in terms of the ratio of optical transparency and radio shielding capabilities.

The shielding mechanism is directly related to the surface resistance of the film and, consequently, to the concentration of AgNW in the sample. Fig. 5, *c, d* shows the histograms of the balance of reflection, transmission, and attenuation for all studied AgNW films in the K- and $K_a$-bands. For example, the absorption is the dominant shielding mechanism (the absorption coefficient is 41.63% in the K-band and 36.9% in the $K_a$-band) in case of films with AgNW concentration of $25\,\mu l$ and the AgNW film is two-dimensional percolated metal mesh. The presence of absorption characteristic of low-conducting structures is similar to the results described in the literature [33] obtained on metallic meshes. We observe a trend towards an increase of the contribution of reflection to the overall shielding efficiency with the increase of the concentration of the base dispersion of AgNW, as the density of AgNW packaging in films increases, and the number of layers increases, which contributes to a strong decrease of surface resistance. For instance, we see the following results in a sample with an AgNW concentration of $1600\,\mu l$: the reflection is 99.7% in the K-band and the reflection is 99.9% in the $K_a$-band.

We decided to use the continuous layer model [34] to compare the radio shielding properties of the obtained AgNW films and this model is described by the following equation

$$SE[dB] = 20\log_{10}\left(1 + \frac{Z_0}{2R}\right), \tag{7}$$

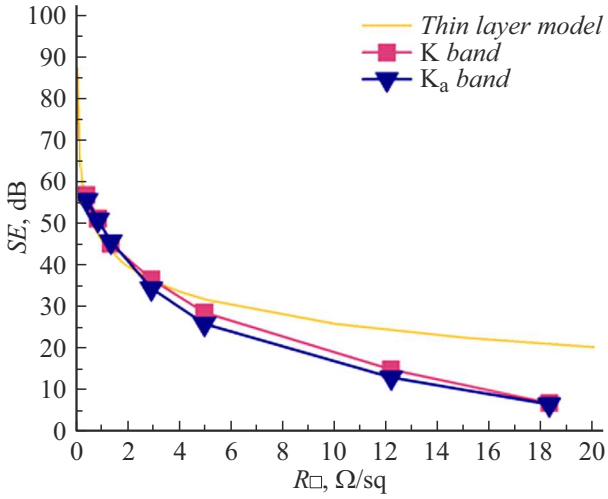


**Figure 6.** Comparison of experimental data with a continuous layer model.

where $Z_0$ is the vacuum impedance, $R$ is the surface resistance of the coating.

Fig. 6 shows a comparison of the data obtained experimentally with the continuous layer model. It shows a high level of agreement for AgNW films with a high concentration of base dispersion ($200-1600\,\mu l$). This is attributable to the fact that such samples have a high packing density and there is a lower probability of defects in the form of large voids, which is an aperture through which wave diffraction can be observed. We see a discrepancy with the continuous layer model with a decrease of the concentration of the base dispersion, since the probability of through defects increases with a decrease of the concentration of AgNW.

### 3.2. Adhesive strength

We mentioned earlier that we integrated AgNW films into RPU. We resorted to the adhesion strength test according to ASTM D4541 to show the degree of resistance to mechanical wear. We made cross-cuts and conducted a tape test for this purpose. The adhesive strength in this test is evaluated using a scoring system: from 0 (almost complete peeling, multiple defects) to 5B (intact state). We see the results of the ASTM D4541 test on Fig. 7. We do not observe peeling, breaks at the edges of the cut and other defects, the films retained their original appearance, which corresponds to the adhesive strength level of 5B (maximum possible) [17].

## Conclusion

We synthesized AgNW with a high aspect ratio in this study and characterized their morphological and structural characteristics. We obtained films from these nanowires by vacuum filtration and then integrated these films into

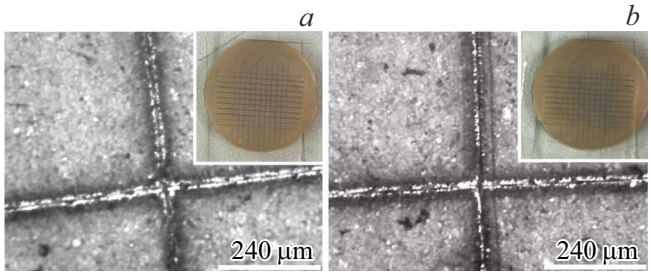


**Figure 7.** Images of adhesion testing sample: *a* — before the adhesive tape is pulled off, *b* — after the adhesive tape is pulled off.

a polyurethane substrate to improve adhesive strength. The dependences of the optical characteristics, namely the transmittance coefficient and the turbidity index, on the volume of the basic AgNW dispersion were determined. A transparent conductive coating with a surface resistance of 4.917,Ω/sq was obtained with an optical transmittance of 69.25%, which makes it potentially applicable for use in optoelectronic applications. Radio shielding properties were studied in a wide frequency range of 18−40 GHz. A sample with a base dispersion concentration of 100,$\mu l$, with a shielding efficiency of more than 25,dB in the K- and $K_a$-bands with an optical transmittance of 69.25% is optimal from the point of view of optoelectric and shielding parameters. The dominant contribution to the shielding mechanism for all types of AgNW films has also been evaluated. It is shown that the dominant shielding mechanism changes from absorption to reflection as the concentration increases.

### Funding

The work for the synthesis, purification and characterization of AgNW and the study of the radio shielding properties of AgNW films in RPU was carried out within the framework of the state assignment of the Ministry of Science and Higher Education of the Russian Federation (topic № FSFN-2024-0016). The optoelectric properties of AgNW films in RPU were studied within the framework of the state assignment of the Ministry of Science and Higher Education of the Russian Federation (topic № FWES-2024-0026).

### Acknowledgments

The studies using scanning and transmission electron microscopy were performed using the equipment of the Krasnoyarsk Regional Center for Collective Use of the Federal Research Center KSC of Siberian Branch of RAS. We would like to thank L.A.Solovyov for his help in X-ray diffraction analysis.

### Conflict of interest

The authors declare that they have no conflict of interest.

## References


[1] S.M. Zachariah, Y. Grohens, N. Kalarikkal, S. Thomas. Polym. Compos., **43**, 2507 (2022). DOI: 10.1002/pc.26595

[2] Z. Chen, C. Xu, C. Ma, W. Ren, H.-M. Cheng. Adv. Mater., **25**, 1296 (2013). DOI: 10.1002/adma.201204196

[3] W. Sihai, D.D.L. Chung. Cem. Concr. Res., **34**, 329 (2004). DOI: 10.1016/j.cemconres.2003.08.014

[4] W. van Eck. Comput. Secur. Comput. Secur., **4**, 269 (1985). DOI: 10.1016/0167-4048(85)90046-X

[5] I. Kubiak, A. Boitan, S. Halunga. Adv. Sci. Inst. Ser. E Appl. Sci., **10**, 2828 (2020). DOI: 10.3390/app10082828

[6] A.S. Voronin, Yu.V. Fadeev, I.V. Govorun, A.S. Voloshin, I.A. Tambasov, M.M. Simunin, S.V. Khartov. Pis'ma v ZhTF, **47** (5), (in Russian). 31 (2021). DOI: 10.21883/PJTF.2021.05.50674.18496

[7] G.M. Olson, J.S. Olson. Annu. Rev. Psychol., **54**, 491 (2003). DOI: 10.1146/annurev.psych.54.101601.145044

[8] D. Tan, C. Jiang, Q. Li, S. Bi, X. Wang, J. Song. J. Mater. Sci.: Mater. Electron., **32**, 25603 (2021). DOI: 10.1007/s10854-021-05409-4

[9] Z. Liang, Z. Zhao, M. Pu, J. Luo, X. Xie, Y. Wang, Y. Guo, X. Ma, X. Luo. Opt. Mater. Express, OME, **10**, 796 (2020). DOI: 10.1364/OME.386830

[10] H. Wang, C. Ji, C. Zhang, Y. Zhang, Z. Zhang, Z. Lu, J. Tan, L.J. Guo. ACS Appl. Mater. Interfaces, **11** (12), 11782 (2019). DOI: 10.1021/acsami.9b00716

[11] Z. Wang, B. Jiao, Y. Qing, H. Nan, L. Huang, W. Wei, Y. Pen, F. Yuan, H. Dong, X. Hou, Z. Wu. ACS Appl. Mater. Interfaces, **12** (2), 2826 (2019). DOI: 10.1021/acsami.9b17513

[12] H. Yang, S. Bai, X. Guo, H. Wang. Appl. Surf. Sci., **483**, 888 (2019). DOI: 10.1016/j.apsusc.2019.04.034

[13] D.H. Kim, Y. Kim, J.-W. Kim. Mater. Des., **89**, 703 (2016). DOI: 10.1016/j.matdes.2015.09.142

[14] R. Sahoo, R. Sundara, V. Subramanian. Mat. Today: Proceed., **94**, 29 (2023). DOI: 10.1016/j.matpr.2023.05.329

[15] L.-C. Jia, D.-X. Yan, X. Liu, R. Ma, H.-Y. Wu, Z.-M. Li. ACS Appl. Mater. Interfaces, **10** (14), 11941 (2018). DOI: 10.1021/acsami.8b00492

[16] I.A. Tambasov, A.S. Voronin, N.P. Evsevskaya, Y.M. Kuznetsov, A.V. Luk'yanenko, E.V. Tambasova, M.O. Gornakov, M.V. Dorokhin, Yu.Yu. Loginov. Phys. Solid State, **62**, 1090 (2020). DOI: 10.1134/S1063783420060311

[17] *Standard Test Method for Pull-off Strength of Coatings Using Portable Adhesion Testers*. https://www.astm.org/d4541-22.html

[18] K.S. Lau, S.X. Chin, S.T. Tan, F.S. Lim, W.S. Chang, C.C. Yap, M.H. Hj Jumali, S. Zakaria, S.W. Chook, C.H. Chia. J. Alloys Compd., **803**, 165 (2019). DOI: 10.1016/j.jallcom.2019.06.258

[19] C.J. Johnson, E. Dujardin, S.A. Davis, C.J. Murphy, S.J. Mann. Mater. Chem., **12**, 1765 (2002). DOI: 10.1039/B200953F

[20] C.S. Todd, X. Chen. Appl. Spectrosc., **74** (2), 204 (2019). DOI: 10.1177/0003702819891060.

[21] Y. Gao, P. Jiang, L. Song, L. Liu, X. Yan, Z. Zhou, D. Liu, J. Wang, H. Yuan, Z. Zhang. J. Phys. D Appl. Phys., **38**, 1061 (2005). DOI: 10.1088/0022-3727/38/7/015

[22] Y. Gao, L. Song, P. Jiang, L.F. Liu, X.Q. Yan, Z.P. Zhou, D.F. Liu, J.X. Wang, H.J. Yuan, Z.X. Zhang, X.W. Zhao, X.Y. Dou, W.Y. Zhou, G. Wang, S.S. Xie, H.Y. Chen, J.Q. Li. J. Cryst. Growth, **276**, 606 (2005). DOI: 10.1016/j.jcrysgro.2004.11.396

[23] Y. Sun, Y. Ren, Y. Liu, J. Wen, J.S. Okasinski, D.J. Miller. Nat. Commun., **3**, 1 (2012). DOI: 10.1038/ncomms1963

[24] G. Khanarian, J. Joo, X.-Q. Liu, P. Eastman, D. Werner, K. O'Connell, P.J. Trefonas. Appl. Phys., **114**, 024302 (2013). DOI: 10.1063/1.4812390

[25] X. Li, J. Zhou, D. Yan, Y. Peng, Y. Wang, Q. Zhou, K. Wang. Materials, **14**, 2219 (2021). DOI: 10.3390/ma14092219

[26] N.H. Mudri, L.C. Abdullah, M.M. Aung, M.Z. Salleh, D.R. Awang Biak, M. Rayung. Polymers, **12**, 1494 (2020). DOI: 10.3390/polym12071494

[27] S. Sorel, P.E. Lyons, S. De, J.C. Dickerson, J.N. Coleman. Nanotechnology, **23**, 185201 (2012). DOI: 10.1088/0957-4484/23/18/185201

[28] S. De, T.M. Higgins, P.E. Lyons, E.M. Doherty, P.N. Nirmalraj, W.J. Blau, J.J. Boland, J.N. Coleman. ACS Nano, **3** (7), 1767 (2009). DOI: 10.1021/nn900348c

[29] R.M. Mutiso, M.C. Sherrott, A.R. Rathmell, B.J. Wiley, K.I. Winey. ACS Nano, **7** (9), 7654 (2013). DOI: 10.1021/nn403324t

[30] A.S. Voronin, F.S. Ivanchenko, M.M. Simunin, A.V. Shiverskiy, A.S. Aleksandrovsky, I.V. Nemtsev, Y.V. Fadeev, D.V. Karpova, S.V. Khartov. Appl. Surf. Sci., **364**, 931 (2016). DOI: 10.1016/j.apsusc.2015.12.182

[31] *IEC 60050 — International Electrotechnical Vocabulary*. https://www.electropedia.org/

[32] H. Wang, S. Li, M. Liu, J. Li, X. Zhou. Macromol. Mater. Eng., **306**, 2100032 (2021). DOI: 10.1002/mame.202100032

[33] S.H. Ryu, Y.K. Han, S.K. Kwon, T. Kim, B.M. Jung, S.-B. Lee, B. Park. Chem. Eng. J., **428**, 131167 (2022). DOI: 10.1016/j.cej.2021.131167

[34] Y. Han, Y. Liu, L. Han, J. Lin, P. Jin. Carbon NY., **115**, 34 (2017).


*Translated by A.Akhtayamov*